Author Manuscript

Author Manuscript

Author Manuscript

Author Manuscript

HHS Public Access

Author manuscript

*Circ Arrhythm Electrophysiol*. Author manuscript; available in PMC 2016 June 01.

Published in final edited form as:

*Circ Arrhythm Electrophysiol*. 2015 June ; 8(3): 667–676. doi:10.1161/CIRCEP.114.002296.

# Small Conductance Calcium-Activated Potassium Current is Important in Transmural Repolarization of Failing Human Ventricles

**Chih-Chieh Yu, MD**[1,2,*], **Christopher Corr, MS**[1,*], **Changyu Shen, PhD**[3,4], **Richard Shelton, MD**[1], **Mrinal Yadava, MD**[1], **Isaac Rhea, MD**[1], **Susan Straka, RN**[1], **Michael C. Fishbein, MD**[5], **Zhenhui Chen, PhD**[1], **Shien-Fong Lin, PhD**[1,6], **John C. Lopshire, MD, PhD**[1,7], and **Peng-Sheng Chen, MD**[1]

[1]Krannert Institute of Cardiology, Division of Cardiology, Department of Medicine, Indiana University School of Medicine, Indianapolis, IN

[3]Department of Biostatistics, Indiana University School of Medicine, Indianapolis, IN

[2]National Taiwan University Hospital, Taipei, Taiwan

[4]Fairbanks School of Public Health, School of Medicine, Indiana University, Indianapolis, IN

[5]Department of Pathology and Laboratory Medicine, David Geffen School of Medicine at UCLA, Los Angeles, CA

[6]Institute of Biomedical Engineering, National Chiao-Tung University, Hsin-Chu, Taiwan

[7]Roudebush Veterans Affairs Medical Center, Indianapolis, IN

## Abstract

**Background—**The transmural distribution of apamin-sensitive small conductance $Ca^{2+}$-activated $K^+$ (SK) current ($I_{KAS}$) in failing human ventricles remains unclear.

**Methods and Results—**We optically mapped left ventricular wedge preparations from 12 failing native hearts and 2 rejected cardiac allografts explanted during transplant surgery. We determined transmural action potential duration (APD) before and after 100 nM apamin administration in all wedges and after sequential administration of apamin, chromanol and E4031 in 4 wedges. Apamin prolonged APD from 363 ms [95% confidence interval (CI), 341 to 385] to 409 [CI, 385 to 434] ($p<0.001$) in all hearts, and reduced the transmural conduction velocity from 36 cm/s [CI, 30 to 42] to 32 cm/s [CI, 27 to 37] ($p=0.001$) in 12 native failing hearts at 1000 ms pacing cycle length (PCL). The percent APD prolongation is negatively correlated with baseline APD and positively correlated with PCL. Only one wedge had M-cell islands. The percentages of APD prolongation in the last 4 hearts at 2000 ms PCL after apamin, chromanol and E4031 were 9.1% [CI, 3.9 to 14.2], 17.3% [CI, 3.1 to 31.5] and 35.9% [CI, 15.7 to 56.1], respectively.

Correspondence: Peng-Sheng Chen, MD, Krannert Institute of Cardiology, Indiana University School of Medicine, 1800 N. Capitol Ave, Room E475, Indianapolis, IN 46202-1228, Tel: (317) 274-0909, Fax: (317) 962-0588, chenpp@iu.edu.

*contributed equally

**Conflict of Interest Disclosures:** None.

Author Manuscript Author Manuscript Author Manuscript Author Manuscript

Immunohistochemical staining of subtype 2 of SK (SK2) protein showed increased expression in intercalated discs of myocytes.

**Conclusions—**SK current is important in the transmural repolarization in failing human ventricles. The magnitude of $I_{KAS}$ is positively correlated with the PCL, but negatively correlated with APD when PCL is fixed. There is abundant SK2 protein in the intercalated discs of myocytes.

### Keywords

action potential; heart failure; ion channel; remodeling; conduction; calcium

Heart failure is associated with significant electrophysiological remodeling that includes a downregulation of most potassium currents and upregulation of late sodium and sodium–calcium exchange currents.[1, 2] These changes reduce the repolarization reserve, prolong the action potential duration (APD) and facilitate the development of ventricular arrhythmias and sudden cardiac death. Small conductance $Ca^{2+}$-activated $K^+$ (SK) current is a repolarization current responsible for afterhyperpolarization of the neurons in the central nervous system.[3–5] Apamin, a western honey bee toxin, is a specific blocker of the SK current in both neurons and cardiac myocytes.[5, 6] Studies from Chiamvimonvat's laboratory showed that apamin-sensitive SK current ($I_{KAS}$) is important in the repolarization of atrial myocytes and play important roles in automaticity and atrioventricular node conduction.[7–9] While $I_{KAS}$ contributes little in the normal ventricles at normal pacing rates,[10] $I_{KAS}$ blockade by apamin can prolong APD in normal ventricles when the pacing rate is slow.[11] More importantly, $I_{KAS}$ is significantly upregulated in myocardial infarction and heart failure. The effects of apamin on APD in diseased hearts also increase with increased pacing cycle length (PCL).[11–17] In addition, blocking $I_{KAS}$ at long PCL may result in spontaneous afterdepolarization, torsades de pointes ventricular arrhythmia and ventricular fibrillation in Langendorff-perfused rabbit hearts.[11] While $I_{KAS}$ is upregulated in diseased hearts, the magnitude of upregulation may vary transmurally. In both failing human and rabbit ventricles, cells isolated from the midmyocardium had lower $I_{KAS}$ density than the cells isolated from the epicardial layer.[12, 13] However, because only a small number of cells were studied, the transmural distribution of $I_{KAS}$ remains unclear. We sought to determine the transmural distribution of $I_{KAS}$ in failing human ventricles by studying the wedge preparation using optical mapping techniques. We also identified the comparative importance of $I_{KAS}$, rapid delayed rectifier potassium current ($I_{Kr}$) and slow delayed rectifier potassium current ($I_{Ks}$) in human ventricles by sequential application of specific blockers. The results are used to test the hypothesis that $I_{KAS}$ inhibition by apamin has significant effects on transmural repolarization in diseased human ventricles.

## Methods

This research project is approved by the Institutional Review Board of the Indiana University Purdue University Indianapolis. We consented and studied 20 consecutive transplant recipients who underwent orthotopic cardiac transplantation. Among them 6 were excluded due to poor signal quality. The remaining 14 were successfully studied (Table 1). A detailed method section can be found in the Data Supplement.

Author Manuscript Author Manuscript Author Manuscript Author Manuscript

### Human Wedge Preparation

A wedge of the left ventricular free wall was perfused by an isolated left circumflex coronary artery branch (Figure 1A). The wedge was Langendorff perfused with 37°C oxygenated Tyrode's solution. Two pseudo-ECG electrodes were mounted on the opposite sides of the wedge. A bipolar pacing lead was hooked onto the endocardium.

### Imaging system: single and dual mapping

For the first 10 hearts, a single camera was used for mapping the action potential (AP). We used blebbistatin to arrest contraction and di-4ANEPPS for voltage mapping. The last 4 hearts were stained with Rhod-2 AM andRH237 for simultaneous AP and calcium transient (CaT) mapping (Figure 1B). The activation time, APD, calcium transient duration (CaTD) and the difference between CaTD and APD (CaTD-APD) of the mapped region were examined (Figure 1C).

### Experimental Protocol

**Protocol I: the effects of apamin on APD—**To determine APD restitution curve before and after apamin, 10 preparations were sequentially paced (in ms) at 2000, 1500, 1000, 900, 800, 700, 600 and 500 PCL. We then determined the steep portion of the APD restitution curve by reducing the PCL from 400 ms in 10 ms steps until loss of capture. Apamin (100 nM) was then added into the perfusate and the protocol was repeated 30 min later.

**Protocol II: The comparative importance of $I_{KAS}$, $I_{Ks}$ and $I_{Kr}$ in ventricular repolarization—**The last 4 hearts were first treated with apamin, followed by chromanol (50 μM) and then E4031 (100 nM). Optical mapping was performed at baseline and after each drug was administered.

### Data processing

The subepicardium and subendocardium were defined by 20% of transmural thickness from epicardium and endocardium, respectively. The remaining 60% of tissue was the midmyocardium. To determine the APD, we selected for analysis four pixels in each layer and obtained a mean of these four pixels to represent the APD of that layer. Transmural APD or CaTD gradients were defined by the difference of APD or CaTD, respectively, between endocardial and epicardial layers.[18] M cell islands were defined as the regions that had longer APD than neighboring myocardium surrounded by a local APD gradient > 15 ms/mm.[18] Transmural conduction time was defined by the difference of activation time between the earliest activation site at endocardium and the corresponding epicardial site. The transmural conduction velocity (TCV) (cm/s) was calculated by the ratio between the transmural thickness and the transmural conduction time. The magnitude of drug-induced changes of APD (% APD prolongation) was calculated by the ratio between the ΔAPD (post-drug APD – pre-drug APD) and the baseline APD.

Immunohistochemical staining was performed using an anti-SK2 rabbit polyclonal antibody (Sigma-Aldrich, St. Louis, MO).[19]

Author Manuscript Author Manuscript Author Manuscript Author Manuscript

### Western blot analysis

Human heart membrane microsomes were obtained by homogenization and centrifugation. Sixty μg of microsomes were subjected to a SDS-polyacrylamide gel electrophoresis and transferred to a nitrocellulose membrane. The blot was probed with a rabbit anti-SK2 polyclonal antibody (Sigma, 1:1000). Antibody-bound protein bands were visualized with 125I-protein A followed by autoradiography.

### Statistical analysis

Results are summarized as mean and 95% confidence interval (CI). Pearson correlation coefficient was used to assess the association between baseline APD and APD prolongation. The paired T tests were used to compare APD, maximal restitution slope and conduction velocity between baseline and post-apamin. Bonferroni method was used to adjust for multiple comparisons. Fisher's exact test was used to compare the occurrence of electrical alternans between baseline and post-apamin. The CI of the proportion of the wedges with strong intercalated discs SK2 staining is based on the exact binomial distribution. Linear mixed-effects models were used to estimate the effects of different drugs averaged over PCL by treating patients as the random effect. All statistical analyses were performed in IBM SPSS Statistics V21 and SAS 9.3 (SAS Inc., Cary, NC). A two sided $p \leq 0.05$ was considered statistically significant.

## Results

### Effects of apamin on transmural APD

Apamin significantly altered transmural APD distribution. Figure 2A and 2B show typical APD maps before and after apamin, respectively, at 2000 ms PCL. Apamin administration prolonged APD throughout the mapped region, as shown by the changing colors between Figures 2A and 2B. Figure 2C shows a significant negative correlation between the magnitudes of APD prolongation and baseline APD. The average correlation coefficient between the magnitudes of APD prolongation and baseline APD in all wedges studied was −0.35 [CI, −0.14 to −0.57] by Pearson correlation (*r*) when PCL was fixed at 2000 ms.

In addition to baseline APD, PCL was also an important factor that determines the magnitudes of APD prolongation after apamin. Figure 3A shows the effects of PCL on APD at 3 different myocardial layers of the wedge preparation, both at baseline and after apamin. Apamin prolonged APD significantly in all three layers at all PCL (p value <0.05 for all). Among them, 22 out of 27 comparisons remained significant after Bonferroni adjustment. The ΔAPD progressively increased with lengthening of PCL. Figure 3B shows the APD restitution curve before and after apamin. Apamin administration increased the maximal slope of APD restitution curve in the subendocardium from 0.49 [CI, 0.41 to 0.57] to 0.58 [CI, 0.48 to 0.69] (p=0.033), but did not significantly change the maximal restitution slope of the subepicardium (from 0.44 [CI, 0.35 to 0.54] to 0.54 [CI, 0.40 to 0.48], p=0.058) or midmyocardium (from 0.42 [CI, 0.35 to 0.50] to 0.51 [CI, 0.41 to 0.61], p=0.096). The observations of electrical alternans when approaching effective refractory periods (ERP) were 6 out of 10 before apamin (ERP=304 ms [CI, 262 to 346]) and 9 out of 10 after apamin (ERP=312 ms [CI 262 to 361]) (p=0.4). No arrhythmia was induced with programmed

Author Manuscript Author Manuscript Author Manuscript Author Manuscript

stimulation before and after apamin in the first two wedges studied. Figure 3C plots the magnitudes of APD prolongation against the PCL at all 3 layers of the myocardium. There was a positive correlation between the magnitudes of APD prolongation and the PCL at all 3 layers (subendocardium, $r$=0.423 [CI, 0.131 to 0.521]; midmyocardium, $r$=0.338 [CI, 0.094 to 0.624]; subepicardium, $r$=0.437 [CI, 0.243 to 0.622]). The differences of APD between subepicardium and subendocardium (the transmural APD gradient) at 1000 ms PCL was 33 ms [CI, 21 to 44] at baseline and 42 ms [CI, 21 to 62] after apamin (p=0.244). The transmural APD gradient correlated positively with PCL both at baseline ($r$=0.816, p=0.007) and after apamin ($r$=0.870, p=0.002) (supplement Figure 1).

There were large individual variations of APD responses to apamin (Figure 3D). A possible mechanism for differential APD response to apamin is pre-transplant treatment with amiodarone, a known inhibitor of $I_{KAS}$.[20] However, the magnitudes of APD prolongation in patients treated with amiodarone (11.6% [CI, −0.5 to 23.7], N=7) did not differ significantly from patients not treated with amiodarone (14.9% [CI, −8.2 to 38.0], N=7) at 1000 ms PCL (p=0.55). None of the other clinical characteristics was significantly associated with APD prolongation induced by apamin (See Supplement Results).

## M cell islands

We applied the criteria used by Glukhov et al[18] to identify the M cell islands in the transmural wedge preparation. Only 1 of 14 wedges had any M cell island according to those criteria. In that wedge, there were two M cell islands at subendocardial and subepicardial regions, respectively, at 2000 ms PCL (red arrows, Figure 4A). The M cell islands had long APD and were surrounded by steep APD gradients. APD in M cell islands averaged 457 ms [CI, 454 to 460], which was increased to 496 ms [95% CI, 495 to 498] after apamin (p<0.001). Figure 4B shows a map of ΔAPD. The M cell islands (red arrows) show less APD prolongation (smaller ΔAPD) than the surrounding tissues. Figure 4C shows the local APD gradients of the mapped area. Red arrows point to the M cell islands surrounded by large local APD gradients. Figure 4D shows the %APD prolongation as a function of baseline APD. There was a highly heterogeneous prolongation of APD when the baseline APD was < 440 ms, with a magnitude of APD prolongation as high as 70%. In contrast, the M cell islands (data points within the red circle) had APD prolongation of only 0–20%, consistent with the observation that the magnitudes of APD prolongation are reversely correlated with the baseline APD. No other wedges had M cell islands detected. When paced at fast rates approaching the ERP, APD alternans was not observed at baseline (Figure 4E, data from points #1 and #2 in Figure 4A). However, after apamin administration, APD alternans was observed in M cell islands (Figure 4F, point #2 in Figure 4A) but not in the tissues outside M cell islands (Figure 4F, point #1 in Figure 4A). The maximal slope of APD restitution curve increased from 0.75 to 1.25 after apamin (Figure 4G and 4H).

## Effects of Apamin on Transmural Conduction Velocity

There was no difference of transmural conduction velocity (TCV) between baseline (37.0 cm/s [CI, 31.5 to 42.3]) and after apamin (35.3 cm/s [CI, 28.8 to 41.8]) (p=0.333) at 1000 ms PCL. Two wedge preparations from rejected cardiac allografts (patients #8 and #14)

Author Manuscript Author Manuscript Author Manuscript Author Manuscript

showed accelerated TCV after apamin (from 43.5 cm/s at baseline [CI, 43.2 to 43.8] to 55.0 cm/s [CI, 54.3 to 55.8]; statistical analysis was not performed due to limited case number). In the remaining 12 patients, the TCV reduced from 35.9 cm/s [CI, 30.1 to 41.7] to 32.0 cm/s [CI, 26.8 to 37.2] (p=0.001). Figure 5A shows the representative activation maps (left panel) and AP tracings (right panel) before and after apamin at 1000 ms PCL. Figure 5B demonstrates the change of TCV at all PCL after the administration of apamin in wedges from either all 14 wedges together (green and blue lines) or from only the 12 wedges from native failing hearts (black and red lines). The reductions of TCV after apamin were significant for the latter group over all PCLs (red line). There was no significant difference between patients with ischemic or non-ischemic cardiomyopathy (−4.0 cm/s [CI, −6.2 to −1.8], n=4 vs. −0.8 cm/s [CI, −3.8 to 2.2], n=10; p=0.132), or in patients with normal (>55%) or abnormal ejection fraction (0.7 cm/s [CI, −7.8 to 9.2], n=3 vs. −2.4 cm/s [CI, −4.6 to −0.1], n=11; p=0.553).

Figure 5C shows the average of local conduction velocity (LCV) in three muscle layers at 1000 ms PCL. There were significant differences among the three muscle layers (p<0.001 when n=14, p=0.004 when n=12). The LCV was the fastest at the subendocardium and the slowest at the midmyocardium. After applying apamin, a significant reduction of LCV was observed at the subendocardium in native hearts (N=12); from 66.9 [CI, 49.4 to 84.3] to 51.7 cm/s [CI, 34.7 to 68.8] (p=0.011). No significant change of LCV was noted in other two layers.

### Immunohistochemical staining

Immunohistochemical staining of the ventricular myocytes showed strong staining of the SK2 protein in the intercalated discs between ventricular myocytes. Figures 5D and 5E are typical examples of the SK2 staining. Figure 5D shows that both the nerves and the myocardium were positively stained with the SK2 protein in patient #4. Figure 5E shows a magnified view of the SK2 proteins in the intercalated discs in patient #5. Strong SK2 staining was found in the intercalated discs of all 14 wedges studied (100% [CI, 80–100]).

### The importance of $I_{KAS}$ relative to $I_{Ks}$, $I_{Kr}$

The effects of apamin, chromanol and E4031 on APD prolongation were studied sequentially in wedges from patients #11–14. Figure 6A shows representative AP tracings from patient #12 at baseline and after sequential administration of apamin, chromanol and E4031. In these 4 hearts, APDs was significantly prolonged by chromanol (p<0.001) and E4031 (p<0.001) when APD prolongation is averaged over different PCL levels. At 2000 ms PCL (Figure 6B), apamin prolonged APD by 9.1% [CI, 3.9 to 14.2], resulting in an increase of APD from 375 ms [CI, 342 to 407] to 409 ms [CI, 366 to 451] (p=0.043). APD increased further by 17.3% [CI, 3.1 to 31.5] to 483 ms [CI, 384 to 581] after addition of chromanol (p=0.111). It further increased by 35.9% [CI, 15.7 to 56.1] to 659 ms [CI, 489 to 828] after addition of E4031 (p=0.04). There were no differences of the magnitudes of APD prolongation among the 3 myocardial layers after the treatment with apamin, chromanol (Figure 6D) or E4031 (Figure 6E). However, the transmural gradient of APD is reduced by E4031 (p=0.0287, including data from all PCL) (Figure 6C). The maximal slope of APD restitution curve of subepicardium, midmyocardium and subendocardium after chromanol

Author Manuscript Author Manuscript Author Manuscript Author Manuscript

are 0.50 [95% CI, 0.33 to 0.67], 0.56 [95% CI, 0.40 to 0.71] and 0.49 [95% CI, 0.37 to 0.61], respectively (p=0.181, p=0.141 and p=0.588, respectively, compared with post apamin); and after E4031 were 1.01 [95% CI, 0.36 to 1.67], 0.90 [95% CI, 0.48 to 1.32] and 0.76 [95% CI, 0.56 to 0.97], respectively (p=0.212, p=0.139 and p=0.049, respectively, compared with post chromanol).

Figure 7A shows representative calcium transient (CaT) tracings and calcium transient duration (CaTD) maps at baseline and after apamin, chromanol and E4031 from patient #12. Apamin did not significantly prolong the CaTD (p=0.502), but chromanol (p=0.042) and E4031 (p<0.001) did. The CaTD prolongation was PCL dependent and was different among drugs. As shown in Figure 7B, the effect of apamin could be observed at long PCLs, while the effect of chromanol was mainly observed at short PCL. There was no significant prolongation of CaTD by apamin in any of the three layers. However, the prolongation of CaTD by chromanol was significant at the subepicardium (p=0.009). E4031 significantly prolonged CaTD in all three layers of the transmural surface, with larger effects at the subepicardium (p=0.004) and midmyocardium (p=0.013) compared to the subendocardium. Therefore, the transmural gradient of CaTD (i.e., CaTD between subendocardium and subepicardium) was eliminated after E4031 (p=0.201) (Figure 7C).

### $I_{KAS}$ and the differences between APD and CaTD

Figure 8A shows the effects of apamin on the difference between CaTD and APD (CaTD-APD) at the subepicardium and the subendocardium from patient #14. Consistent with that reported by Lou et al,[21] there was a larger CaTD-APD at the subendocardium than at the subepicardium or midmyocardium (p<0.001 for both comparisons). This difference increased with increasing PCL (Figure 8B). Apamin significantly (p<0.001) reduced the CaTD-APD on the subendocardium but not in the midmyocardium (p=0.141) or the subepicardium (p=0.146) (Figure 8C). This differential effect resulted in a reduction, but not elimination, of the differences of CaTD-APD between subendocardium and the other two layers (p=0.078 compared to midmyocardium; p<0.001 compared to subepicardium). CaTD-APD is further reduced by chromanol (p<0.001,) and E4031 (p<0.001), resulting in the elimination of the differential CaTD-APD among the three layers after all 3 drugs were given (supplement Figures 2 and 3).

## Discussion

The major finding of our study is that $I_{KAS}$ is important in the repolarization of the transmural wedge preparation in failing human ventricles. The conclusion is strengthened by our recent study that showed apamin is a highly specific SK current blocker.[6] The magnitude of $I_{KAS}$ was positively correlated with the PCL. At a fixed PCL, the magnitude of $I_{KAS}$ was negatively correlated with APD. The M cells (which have long APDs) appear to have less $I_{KAS}$ upregulation than the non-M cells. We also found that there was an abundant expression of SK2 proteins in the intercalated discs, and that apamin may reduce transmural conduction velocity in native failing ventricles but not in the ventricles removed due to rejection. Finally, the presence of $I_{KAS}$ may be in part responsible for the differences between CaTD and APD in the failing ventricles.

Author Manuscript Author Manuscript Author Manuscript Author Manuscript

### $I_{KAS}$ and transmural repolarization in human wedge preparation

We showed that the transmural APD significantly and heterogeneously prolonged when exposed to apamin. However, previous studies from our laboratory found a lower $I_{KAS}$ density in cells isolated from the midmyocardial layer than that isolated from subepicardial and subendocardial layers in failing rabbit and human ventricles.[12, 13] In comparison, we found no statistically significant differences of apamin-induced APD changes among the three myocardial layers. These findings may be explained by the effects of electrical coupling which may reduce the transmural repolarization heterogeneity in the wedge preparation compared with that in isolated myocytes.[2223]

### The APD and the PCL

At a fixed PCL, there is a clear negative correlation between the magnitude of apamin-induced APD prolongation and the baseline APD. These findings imply that $I_{KAS}$ upregulation is important in maintaining transmural repolarization reserve. Failure to upregulate $I_{KAS}$ is a characteristic finding in cells with long APDs. If the APD is the only determinant for apamin-responsiveness, then conditions that typically lengthen APD (such as long PCL) should be associated with reduced apamin responsiveness. However, lengthening PCL in the human wedge preparation significantly increased the magnitude of APD prolongation induced by apamin. The K channel blockers (class III antiarrhythmic agents) are known to exhibit reverse use-dependence, resulting in greater prolongation of APD at longer PCL.[24] Apamin may have similar reverse use-dependent properties, resulting in greater effects on $I_{KAS}$ at longer PCL. Reverse use-dependence may also underlie that proarrhythmic effects of apamin at slow ventricular rates.[11]

### $I_{KAS}$ and the characteristics of M cells

The M cell is distinguished from other ventricular myocytes based on the ability of its APD to prolong prominently at slower rates.[25] Distinct M cell islands are observed frequently in the wedge preparation from normal ventricles but rarely in failing ventricles.[18, 21] Consistent with these previous studies, we found only two M cell islands in one of the 14 wedges studied. In that M cell island, APD is long and the magnitude of APD prolongation induced by apamin is small. These data suggest that M cells in failing ventricles are characterized by a deficiency in $I_{KAS}$ as compared with most of the surrounding myocytes. When the PCL is lengthened, the repolarization reserve of non-M cells is maintained in part by a robust upregulation of the $I_{KAS}$. However, because of the relative deficiencies of the $I_{KAS}$ in the M cell island, it was not able to maintain its repolarization reserve thus prolonged its APD more prominently during the slow than the fast rates. This phenomenon (the ability for APD to prolong prominently at slower rates) fulfills the traditional definition of M cell.[25]

While M cell islands have longer APD than the surrounding tissues, no electrical alternans were observed when PCL shortened to near ERP. After apamin administration, the M cell island and the surrounding tissues had similar APD. However, rapid pacing induced electric alternans only in the M cell island. While $I_{KAS}$ is not prominently upregulated in M cell islands, it may still play an important role in preventing alternans at fast rates. $I_{KAS}$ blockade may have larger effects on the repolarization reserve of the M cell islands than the surrounding myocardium.

Author Manuscript Author Manuscript Author Manuscript Author Manuscript

### $I_{KAS}$ and transmural conduction

We found that apamin prolonged transmural conduction time in 12 wedges isolated from failing native hearts. There is also abundant SK2 protein in the intercalated discs, suggesting that apamin may significantly interfere with the intercalated disc function. Previous studies have shown that SK2 channel knockout in a murine model results in prolongation of the PR interval and that the $SK2^{\Delta/\Delta}$ mice may develop complete atrioventricular block.[9] Studies in mice resistance arteries showed that electrical conduction along the endothelium of the arteries is also controlled in part by the SK2.[26] Other investigators showed that overexpression of SK3 in murine model is associated with reduced ventricular conduction velocity, bradyarrhythmias, heart block and sudden death.[27] These findings imply a possible role of SK channels in cell-cell signal transduction and conduction.

### The relative importance of $I_{KAS}$, $I_{Ks}$ and $I_{Kr}$

The magnitude of APD prolongation after apamin varies greatly from site to site. In some locations, the APD could prolong up to 70% after apamin administration. Previous reports about the $I_{Ks}$ and $I_{Kr}$ in transmural preparations were mostly performed in canine models using pharmacological interventions. Because E4031 and chromanol 293 also blocks the SK current,[20] APD prolongation in those studies may be in part due to the inhibition of the SK currents. In our study, we gave apamin first, followed by chromanol 293 and E4031. Our results did not show different magnitudes of APD prolongation by potassium channel blockers in different myocardial layers.

### $I_{KAS}$ and CaTD-APD

We found an increased CaTD-APD in the transmural wedge. The magnitudes of CaTD-APD are the largest at the subendocardium, a finding consistent with earlier studies in failing human hearts.[21] The CaTD-APD was reduced by apamin, suggesting that $I_{KAS}$ upregulation in failing ventricles is in part responsible for differences between CaTD and APD.

### The SK subtypes

The SK channels have 3 different subtypes: SK1, SK2 and SK3.[28] Among them, SK2 is most sensitive to apamin, followed by SK3 and SK1, respectively.[29] SK1 sensitivity to apamin is species-specific and that SK1 in humans is apamin sensitive.[29] Because we used high dose (100 nM) of apamin in this study, all 3 subtypes of SK currents should have been blocked during the drug administration. However, it is not possible to determine the relative importance of these 3 subtypes of SK currents in the conduction and repolarization in the human transmural wedge preparations. Our earlier study had detected only a small amount of SK3 protein in the normal and failing human ventricles.[13] In contrast, the SK2 protein is abundantly present in failing human ventricles and is most sensitive to apamin. Therefore, we have focused our study on SK2.

## Limitations

There are several limitations in this study. First, the etiology and duration of disease varied greatly among the subjects of the study. Nine of them had received ventricular assist device before receiving transplantation. Four of them received cardiac resynchronization therapy

Author Manuscript Author Manuscript Author Manuscript Author Manuscript

before transplantation. Both forms of therapy may result in ventricular remodeling. Second, we attempted to map 20 hearts between January 2012 and December 2013, but only 14 hearts were successfully studied and included in this analysis. Various technical issues might have been involved in failed mapping studies, but it remains possible that the hearts not successfully mapped may have different SK currents than the hearts successfully mapped. Third, the number of patients in the second part of the experiment is small, although the results among these 4 ventricles consistently showed that all 3 major K channels played important roles in ventricular repolarization. One of the 4 hearts was from a patient with cardiac allograft rejection. The number of patients is too small to determine if that heart had a different drug response than the other 3 hearts. Fourth, we only studied left ventricular free wall, perfused by a branch of left circumflex artery. Therefore, the finding in this study may not apply to other regions of the ventricles. Finally, the photosensitive dyes and the electromechanical uncoupler may have electrophysiological effects that affect the results of the study.

## Conclusions

We conclude that $I_{KAS}$ is important in the transmural repolarization in diseased human ventricles. The magnitude of $I_{KAS}$ is positively correlated with the PCL, but negatively correlated with APD when PCL is fixed. There is abundant SK2 protein in the intercalated discs. These results suggest that SK current may be an important new target for antiarrhythmic drug therapy.

## Supplementary Material

Refer to Web version on PubMed Central for supplementary material.

## Acknowledgments

We thank Drs. Thomas Wozniak, Mark Turrentine and John Brown for their effort to collect the hearts; we thank Jian Tan, Jessica Warfel and Glen Schmeisser for their assistance in lab procedures.

**Funding Sources:** This study was supported in part by NIH Grants P01 HL78931, R01 HL71140, R41 HL124741 a Medtronic-Zipes Endowment (PSC), the Indiana University Health-Indiana University School of Medicine Strategic Research Initiative, and by an endowment from the Piansky Family Trust (MCF).

## References

1. Aiba T, Tomaselli GF. Electrical remodeling in the failing heart. Curr Opin Cardiol. 2010; 25:29–36. [PubMed: 19907317]
2. Nattel S, Maguy A, Le Bouter S, Yeh YH. Arrhythmogenic ion-channel remodeling in the heart: heart failure, myocardial infarction, and atrial fibrillation. Physiol Rev. 2007; 87:425–456. [PubMed: 17429037]
3. Kohler M, Hirschberg B, Bond CT, Kinzie JM, Marrion NV, Maylie J, Adelman JP. Small-conductance, calcium-activated potassium channels from mammalian brain. Science. 1996; 273:1709–1714. [PubMed: 8781233]
4. Allen D, Bond CT, Lujan R, Ballesteros-Merino C, Lin MT, Wang K, Klett N, Watanabe M, Shigemoto R, Stackman RW Jr, Maylie J, Adelman JP. The SK2-long isoform directs synaptic localization and function of SK2-containing channels. Nat Neurosci. 2011; 14:744–749. [PubMed: 21602822]

Author Manuscript Author Manuscript Author Manuscript Author Manuscript


5. Adelman JP, Maylie J, Sah P. Small-conductance Ca2+-activated K+ channels: form and function. Annu Rev Physiol. 2012; 74:245–269. [PubMed: 21942705]
6. Yu CC, Ai T, Weiss JN, Chen PS. Apamin Does Not Inhibit Human Cardiac Na+ Current, L-type Ca2+ Current or Other Major K+ Currents. PLoS One. 2014; 9:e96691. [PubMed: 24798465]
7. Xu Y, Tuteja D, Zhang Z, Xu D, Zhang Y, Rodriguez J, Nie L, Tuxson HR, Young JN, Glatter KA, Vazquez AE, Yamoah EN, Chiamvimonvat N. Molecular identification and functional roles of a Ca(2+)-activated K+ channel in human and mouse hearts. J Biol Chem. 2003; 278:49085–49094. [PubMed: 13679367]
8. Tuteja D, Rafizadeh S, Timofeyev V, Wang S, Zhang Z, Li N, Mateo RK, Singapuri A, Young JN, Knowlton AA, Chiamvimonvat N. Cardiac small conductance Ca2+-activated K+ channel subunits form heteromultimers via the coiled-coil domains in the C termini of the channels. Circ Res. 2010; 107:851–859. [PubMed: 20689065]
9. Zhang Q, Timofeyev V, Lu L, Li N, Singapuri A, Long MK, Bond CT, Adelman JP, Chiamvimonvat N. Functional roles of a Ca2+-activated K+ channel in atrioventricular nodes. Circ Res. 2008; 102:465–471. [PubMed: 18096820]
10. Nagy N, Szuts V, Horvath Z, Seprenyi G, Farkas AS, Acsai K, Prorok J, Bitay M, Kun A, Pataricza J, Papp JG, Nanasi PP, Varro A, Toth A. Does small-conductance calcium-activated potassium channel contribute to cardiac repolarization? J Mol Cell Cardiol. 2009; 47:656–663. [PubMed: 19632238]
11. Chang PC, Hsieh YC, Hsueh CH, Weiss JN, Lin SF, Chen PS. Apamin induces early afterdepolarizations and torsades de pointes ventricular arrhythmia from failing rabbit ventricles exhibiting secondary rises in intracellular calcium. Heart Rhythm. 2013; 10:1516–1524. [PubMed: 23835258]
12. Chua SK, Chang PC, Maruyama M, Turker I, Shinohara T, Shen MJ, Chen Z, Shen C, Rubart-von der Lohe M, Lopshire JC, Ogawa M, Weiss JN, Lin SF, Ai T, Chen PS. Small-conductance calcium-activated potassium channel and recurrent ventricular fibrillation in failing rabbit ventricles. Circ Res. 2011; 108:971–979. [PubMed: 21350217]
13. Chang PC, Turker I, Lopshire JC, Masroor S, Nguyen BL, Tao W, Rubart M, Chen PS, Chen Z, Ai T. Heterogeneous upregulation of apamin-sensitive potassium currents in failing human ventricles. J Am Heart Assoc. 2013; 2:e004713. [PubMed: 23525437]
14. Hsieh YC, Chang PC, Hsueh CH, Lee YS, Shen C, Weiss JN, Chen Z, Ai T, Lin SF, Chen PS. Apamin-sensitive potassium current modulates action potential duration restitution and arrhythmogenesis of failing rabbit ventricles. Circ Arrhythm Electrophysiol. 2013; 6:410–418. [PubMed: 23420832]
15. Bonilla IM, Long VP 3rd, Vargas-Pinto P, Wright P, Belevych A, Lou Q, Mowrey K, Yoo J, Binkley PF, Fedorov VV, Gyorke S, Janssen PM, Kilic A, Mohler PJ, Carnes CA. Calcium-activated potassium current modulates ventricular repolarization in chronic heart failure. PLoS One. 2014; 9:e108824. [PubMed: 25271970]
16. Lee YS, Chang PC, Hsueh CH, Maruyama M, Park HW, Rhee KS, Hsieh YC, Shen C, Weiss JN, Chen Z, Lin SF, Chen PS. Apamin-Sensitive Calcium-Activated Potassium Currents in Rabbit Ventricles with Chronic Myocardial Infarction. J Cardiovasc Electrophysiol. 2013; 24:1144–1153. [PubMed: 23718850]
17. Gui L, Bao Z, Jia Y, Qin X, Cheng ZJ, Zhu J, Chen QH. Ventricular tachyarrhythmias in rats with acute myocardial infarction involves activation of small-conductance Ca2+-activated K+ channels. Am J Physiol Heart Circ Physiol. 2013; 304:H118–130. [PubMed: 23086994]
18. Glukhov AV, Fedorov VV, Lou Q, Ravikumar VK, Kalish PW, Schuessler RB, Moazami N, Efimov IR. Transmural dispersion of repolarization in failing and nonfailing human ventricle. Circ Res. 2010; 106:981–991. [PubMed: 20093630]
19. Shen MJ, Hao-Che C, Park HW, George Akingba A, Chang PC, Zheng Z, Lin SF, Shen C, Chen LS, Chen Z, Fishbein MC, Chiamvimonvat N, Chen PS. Low-level vagus nerve stimulation upregulates small conductance calcium-activated potassium channels in the stellate ganglion. Heart Rhythm. 2013; 10:910–915. [PubMed: 23357541]
20. Turker I, Yu CC, Chang PC, Chen Z, Sohma Y, Lin SF, Chen PS, Ai T. Amiodarone inhibits apamin-sensitive potassium currents. PLoS One. 2013; 8:e70450. [PubMed: 23922993]

Author Manuscript Author Manuscript Author Manuscript Author Manuscript

21. Lou Q, Fedorov VV, Glukhov AV, Moazami N, Fast VG, Efimov IR. Transmural heterogeneity and remodeling of ventricular excitation-contraction coupling in human heart failure. Circulation. 2011; 123:1881–1890. [PubMed: 21502574]
22. Yan GX, Shimizu W, Antzelevitch C. Characteristics and distribution of M cells in arterially perfused canine left ventricular wedge preparations. Circulation. 1998; 98:1921–1927. [PubMed: 9799214]
23. Myles RC, Bernus O, Burton FL, Cobbe SM, Smith GL. Effect of activation sequence on transmural patterns of repolarization and action potential duration in rabbit ventricular myocardium. Am J Physiol Heart Circ Physiol. 2010; 299:H1812–1822. [PubMed: 20889843]
24. Hondeghem LM, Snyders DJ. Class III antiarrhythmic agents have a lot of potential but a long way to go. Reduced effectiveness and dangers of reverse use dependence. Circulation. 1990; 81:686–690. [PubMed: 2153477]
25. Antzelevitch C. M cells in the human heart. Circ Res. 2010; 106:815–817. [PubMed: 20299671]
26. Behringer EJ, Shaw RL, Westcott EB, Socha MJ, Segal SS. Aging impairs electrical conduction along endothelium of resistance arteries through enhanced Ca2+-activated K+ channel activation. Arterioscler Thromb Vasc Biol. 2013; 33:1892–1901. [PubMed: 23723370]
27. Mahida S, Mills RW, Tucker NR, Simonson B, Macri V, Lemoine MD, Das S, Milan DJ, Ellinor PT. Overexpression of KCNN3 results in sudden cardiac death. Cardiovasc Res. 2014; 101:326–334. [PubMed: 24296650]
28. Tuteja D, Xu D, Timofeyev V, Lu L, Sharma D, Zhang Z, Xu Y, Nie L, Vazquez AE, Young JN, Glatter KA, Chiamvimonvat N. Differential expression of small-conductance Ca2+-activated K+ channels SK1, SK2, and SK3 in mouse atrial and ventricular myocytes. Am J Physiol Heart Circ Physiol. 2005; 289:H2714–2723. [PubMed: 16055520]
29. Weatherall KL, Seutin V, Liegeois JF, Marrion NV. Crucial role of a shared extracellular loop in apamin sensitivity and maintenance of pore shape of small-conductance calcium-activated potassium (SK) channels. Proc Natl Acad Sci U S A. 2011; 108:18494–18499. [PubMed: 22025703]

Author Manuscript Author Manuscript Author Manuscript Author Manuscript

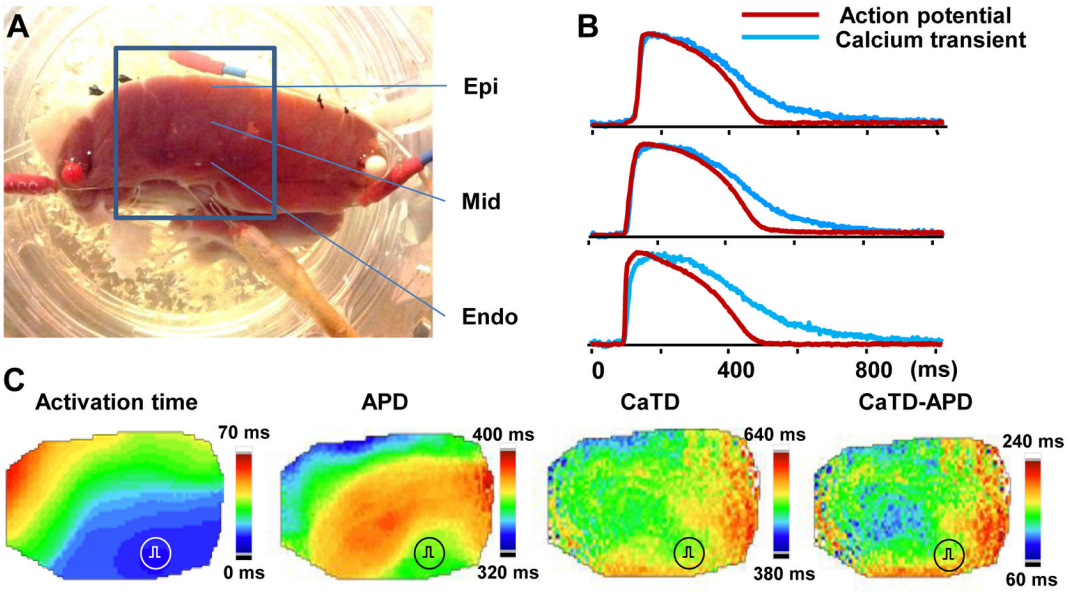


**Figure 1.**

Optical mapping of the left ventricular wedge preparation. **A,** A typical left ventricular wedge preparation. A blue square marks the mapped area (camera field of view). **B,** Representative action potential and intracellular calcium transient tracings. **C,** Examples of 2-dimensional distribution of the activation time, APD, CaTD and CaTD-APD. Data came from patient #14 at 2000 ms PCL. APD, action potential duration; CaTD, calcium transient duration; CaTD-APD, difference between CaTD and APD; Endo, subendocardial layer; Epi, subepicardial layer; Mid, midmyocardial layer.

Author Manuscript Author Manuscript Author Manuscript Author Manuscript

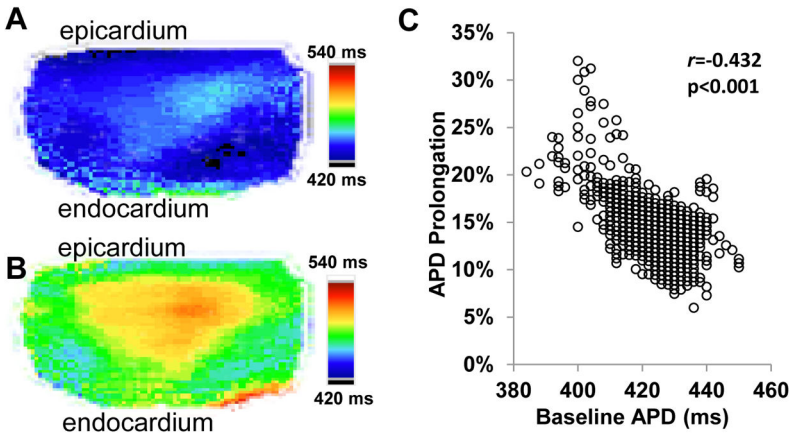


**Figure 2.**

Effects of apamin on transmural APD distribution. The wedge was from patient #10 and was paced at 2000 ms from the endocardium. **A,** APD distribution at baseline. **B,** APD distribution after apamin. **C,** X-Y scatter plots showing that the magnitude of APD prolongation is negatively correlated with the baseline APD. *r* represents Pearson correlation coefficient.

Author Manuscript Author Manuscript Author Manuscript Author Manuscript

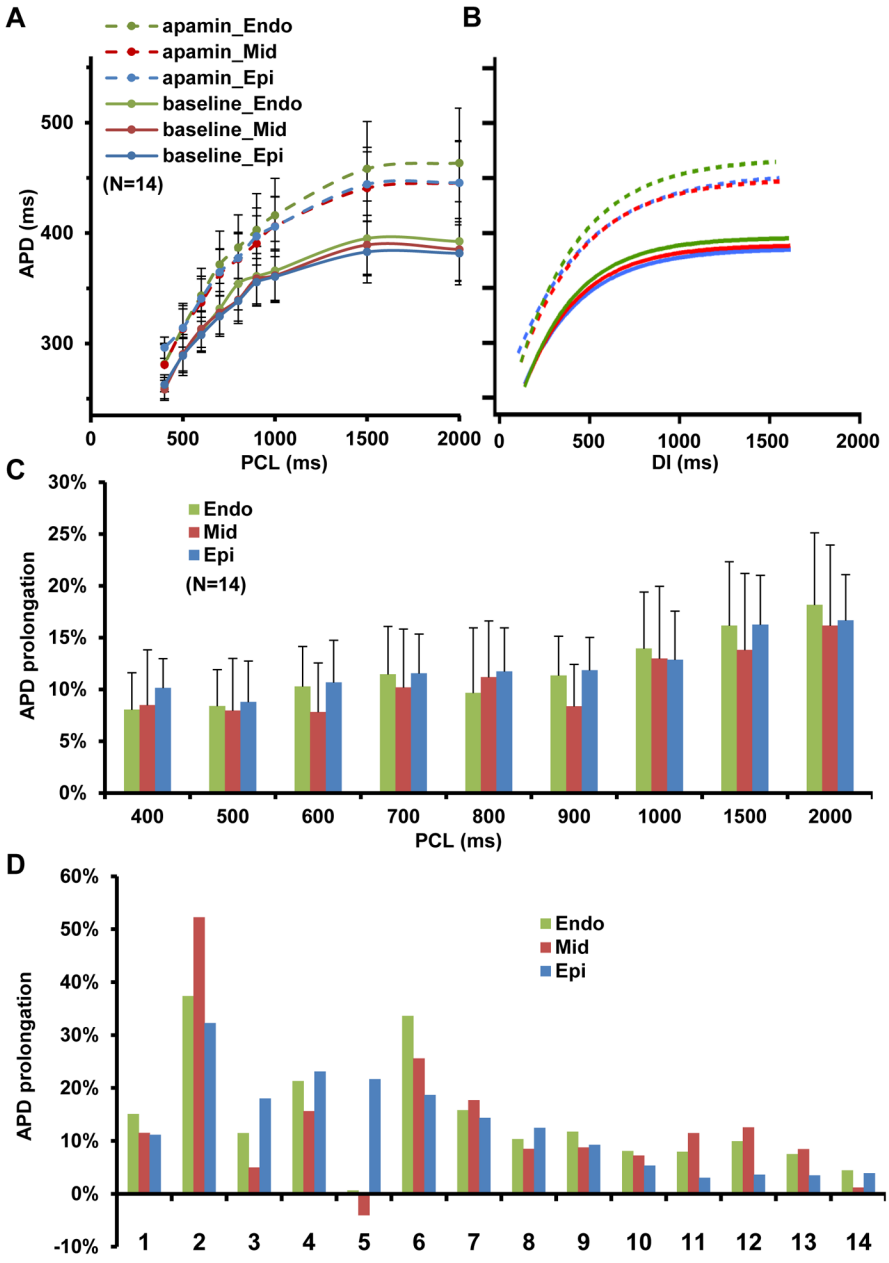


**Figure 3.**

Effects of apamin on APD prolongation over different PCLs and transmural locations. **A,** Transmural APD distribution at baseline and after apamin. APD after apamin (dotted lines) at each layer was significantly ($p<0.05$) longer than APD at baseline (solid lines) in the same layer. **B,** Restitution curves at baseline and after apamin. **C,** APD prolongation at different PCLs. **D,** APD prolongation in each patient. Bars represent 95% confidence interval. DI, diastolic interval; Endo, subendocardial layer; Epi, subepicardial layer; Mid, midmyocardial layer.

Author Manuscript Author Manuscript Author Manuscript Author Manuscript

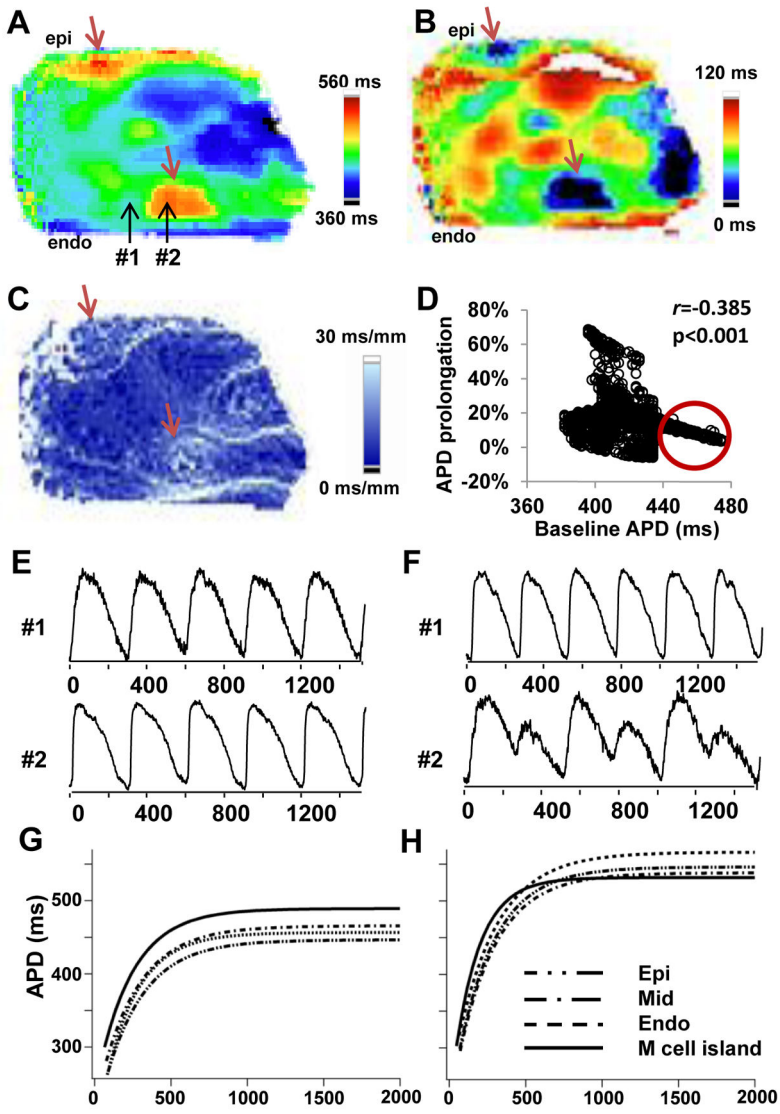


**Figure 4.**

Effects of apamin in M cell islands (patient #4). **A,** APD distribution map at baseline at 2000 ms PCL. Red arrows indicate M cell islands. Black arrows indicate the locations where the representative tracings shown in (E) were censored. **B,** ΔAPD map showing the difference of APD between baseline and after apamin at 2000 ms PCL. **C,** Local APD gradient map at baseline at 2000 ms PCL. **D,** X-Y scatter plots showing APD prolongation vs. baseline APD. The red circle highlights regions with the longest baseline APD (M cells) at 2000 ms PCL. **E,** Action potential tracings at baseline at regions #1 and #2 in (A) at 300 ms PCL. **F,** Action potential tracings of the same pixels as figure E after apamin at 260 ms PCL. **G,** Restitution curves of three muscle layers and M cell islands. **H,** Restitution curves after apamin. DI, diastolic interval; Endo, subendocardial layer; Epi, subepicardial layer; Mid, midmyocardial layer.

Author Manuscript Author Manuscript Author Manuscript Author Manuscript

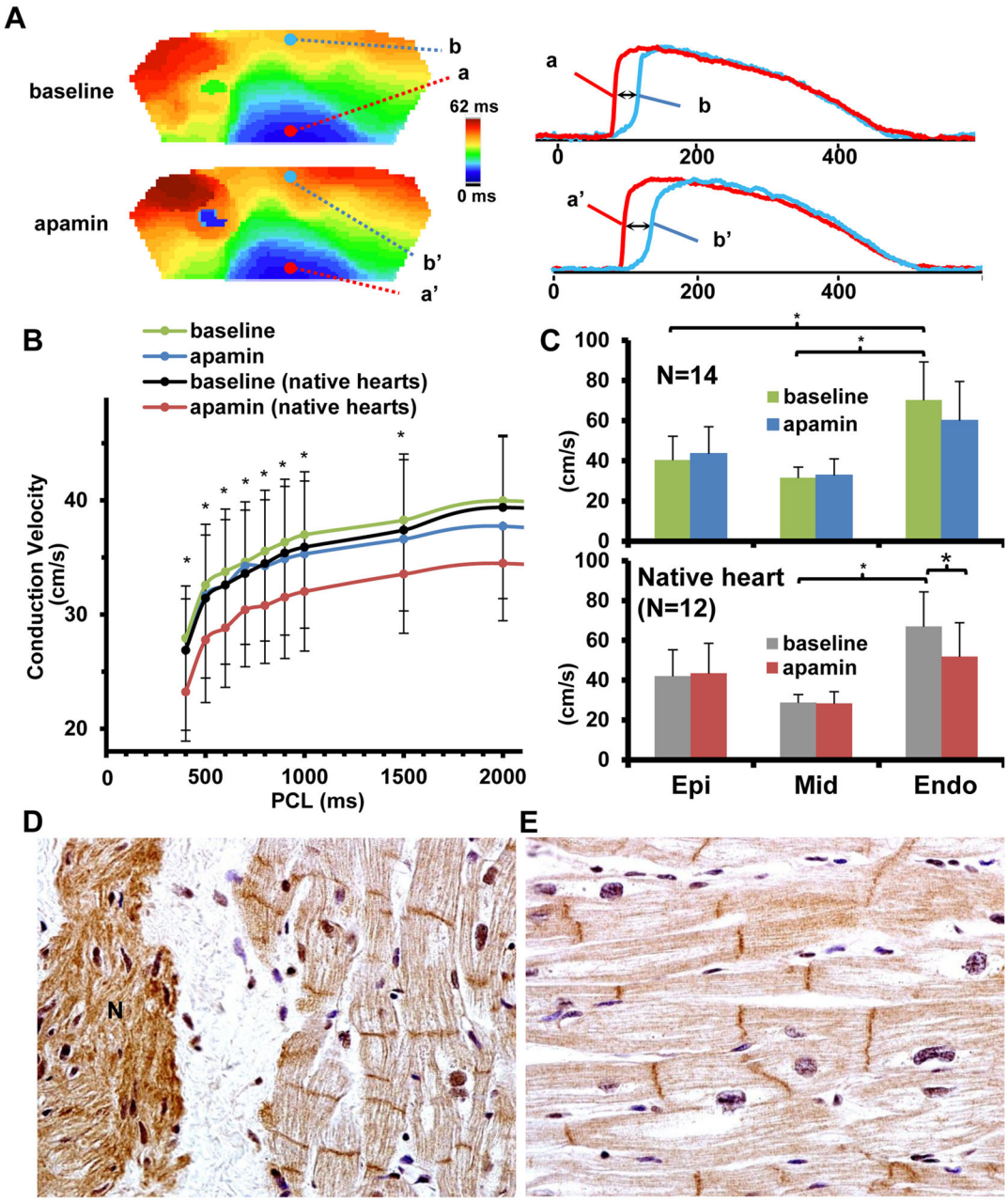


**Figure 5.**

Effects of apamin on transmural conduction velocity. **A,** Representative activation maps at baseline and after apamin from patient #5 at 1000 ms PCL. Red and blue dots mark the sites where representatives on the right were obtained. **B,** The estimated transmural conduction velocity restitution curves of all wedges (n=14) and wedges from native hearts (n=12) before and after apamin. *p<0.05 between baseline and apamin in native hearts (n=12). **C,** The conduction velocity at three different myocardial layers of all hearts (upper panel) and native hearts (lower panel) at 1000 ms PCL. **D,** Immunohistochemical staining of SK2 protein from endocardial layer of wedge #5. The staining was strongest at the nerve (N) and the intercalated discs of the myocytes (200x magnification). **E,** Immunohistochemical

staining of SK2 protein from the epicardial layer in wedge #4 (400x magnification). Bars represent 95% confidence interval. Endo, subendocardial layer; Epi, subepicardial layer; Mid, midmyocardial layer.

Author Manuscript Author Manuscript Author Manuscript Author Manuscript

Author Manuscript Author Manuscript Author Manuscript Author Manuscript

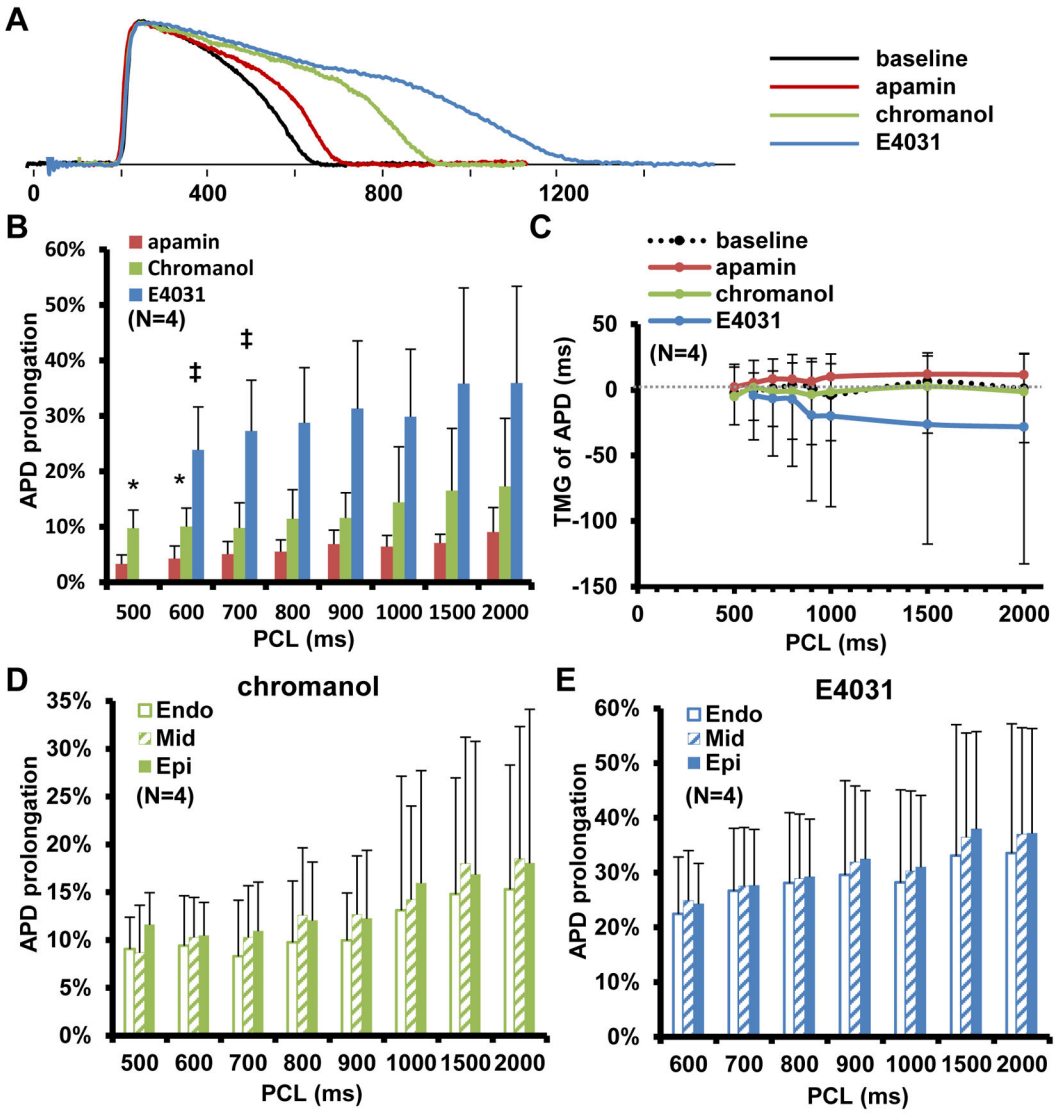


**Figure 6.**

Comparison of APD prolongation by apamin, chromanol and E4031. **A,** Representative action potential tracings from patient #12 at baseline, after apamin, chromanol and E4031 at 2000 ms PCL. **B,** The percentage of APD prolongation by apamin, chromanol and E4031. *p<0.05 comparing the effect of apamin and chromanol. †p<0.05 comparing the effect of chromanol and E4031. **C,** Transmural APD gradients at different PCL. **D,** Effects of chromanol on APD in three myocardial layers. **E,** Effects of E4031 on APD in three myocardial layers. Bars represent 95% confidence interval. Endo, subendocardial layer; Epi, subepicardial layer; Mid, midmyocardial layer.

Author Manuscript Author Manuscript Author Manuscript Author Manuscript

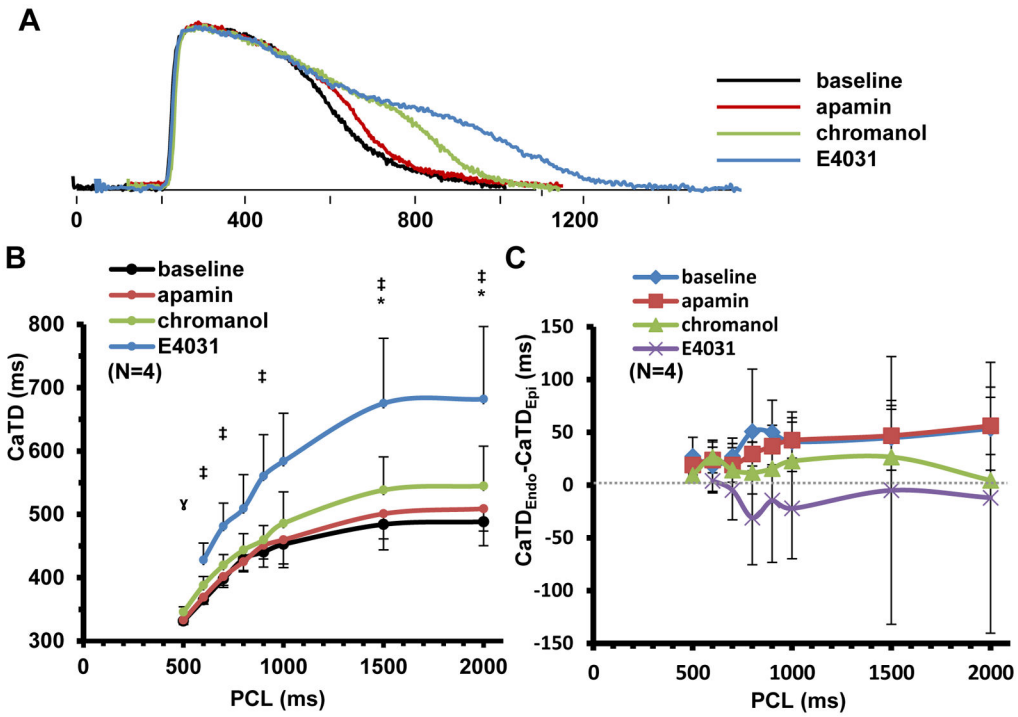


**Figure 7.**

Effects of apamin, chromanol and E4031 on CaTD. **A,** Representative calcium transient tracings and CaTD maps from patient #12 at 2000 ms PCL at baseline and after sequential administration of apamin, chromanol and E4031. **B,** CaTD at different PCL. *p<0.05 between baseline CaTD and that after apamin. †p<0.05 between after apamin and after chromanol. ‡p<0.05 between after chromanol and after E4031. **C,** transmural gradient of CaTD at different PCLs. Bars represent 95% confidence interval. CaTD, calcium transient duration.

Author Manuscript Author Manuscript Author Manuscript Author Manuscript

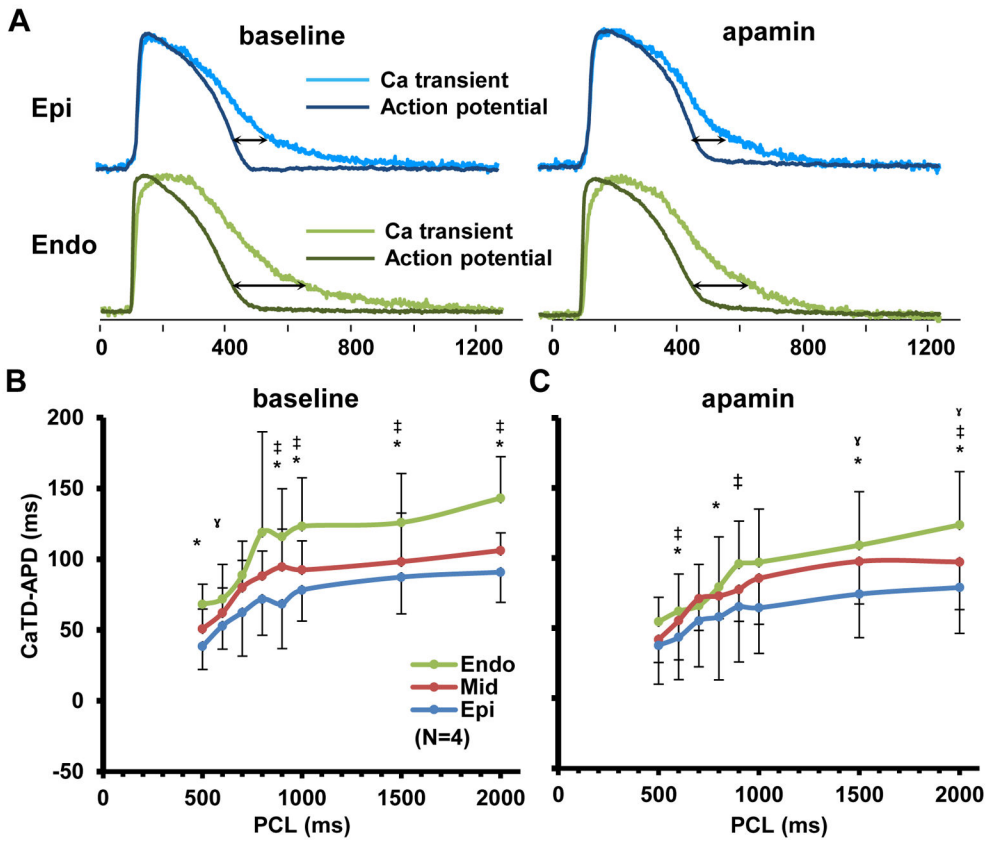


**Figure 8.**

CaTD-APD at baseline and after sequential administration of apamin, chromanol and E4031. **A,** Representative action potential and calcium transient tracings at subendocardium and subepicardium from patient #14 at baseline and after apamin at 2000 ms PCL. **B,** CaTD-APD of three myocardial layers at baseline. **C,** CaTD-APD of three muscle layers after apamin. *p<0.05 when comparing CaTD-APD at the subendocardium and the subepicardium. †p<0.05 when comparing CaTD-APD at the subendocardium and the midmyocardium. ‡p<0.05 when comparing CaTD-APD at the midmyocardium and the subepicardium. Bars represent 95% confidence interval. CaTD-APD, difference between calcium transient duration and action potential duration; Endo, subendocardial layer; Epi, subepicardial layer; Mid, midmyocardial layer.

Author Manuscript Author Manuscript Author Manuscript Author Manuscript





*Circ Arrhythm Electrophysiol*. Author manuscript; available in PMC 2016 June 01.

**Table 1**

Clinical characteristics

| No. | Age | Gender | Etiology | Regional wall motion abnormality | LVEF before VAD | LVEF before transpl | VAD | CRT | Drug | %APD | ΔTCV (cm/s) | Experiment |
|---|---|---|---|---|---|---|---|---|---|---|---|---|
| 1 | 62 | M | Ischemic CM | Global LV hypokinesis | 20 | 18 | + | | A | 12.7% | −3.5 | AP, IHC |
| 2 | 59 | M | Non-ischemic CM: alcoholic | Global LV hypokinesis | 20 | 34 | + | + | B | 40.5% | 0.0 | AP, IHC |
| 3 | 57 | F | Non-ischemic CM/ familial dilated CM | Global LV hypokinesis | 15 | 25 | + | | | 11.7% | −2.3 | AP, IHC |
| 4 | 58 | M | Non-ischemic CM/ idiopathic dilated CM | Global LV hypokinesis | 20 | 23 | + | | B | 19.9% | −2.4 | AP, IHC |
| 5 | 45 | M | Non-ischemic CM/ familial dilated CM | Global LV hypokinesis | - | 31 | | | A,B | 6.5% | −5.0 | AP, IHC |
| 6 | 66 | M | Non-ischemic CM/ idiopathic dilated CM | anterior and posterior wall hypokinesia | - | 17 | | | A | 25.6% | −4.3 | AP, IHC |
| 7 | 69 | M | Ischemic CM | mid anterior septum, apical septum and apex severely hypo to akinetic | 14 | 57 | + | | | 16.0% | −1.7 | AP, IHC |
| 8 | 62 | M | Rejected cardiac allograft | Global LV hypokinesis | - | 20 | | + | A | 10.4% | 9.3 | AP, IHC |
| 9 | 59 | M | Non-ischemic CM/ myotonic dystrophy type 2 | Global LV hypokinesis | 10 | 18 | + | + | A,B | 9.9% | −4.5 | AP, IHC |
| 10 | 59 | M | Non-ischemic CM/ restrictive CM | No regional wall motion abnormalities | - | 56 | | | | 6.9% | −5.2 | AP, IHC |
| 11 | 41 | M | Ischemic CM | Global LV hypokinesis | 15 | 12 | + | | A | 7.4% | −6.1 | AP, CaT, IHC |
| 12 | 54 | M | Non-ischemic CM/ idiopathic dilated CM | Global LV hypokinesis | 20 | 30 | + | + | A | 8.6% | −2.7 | AP, CaT, IHC |
| 13 | 59 | F | Ischemic CM | Global LV hypokinesis and apical akinesia | 24 | 26 | + | | B | 6.4% | −4.5 | AP, CaT, IHC |
| 14 | 32 | M | Rejected cardiac allograft | Restrictive filling pattern | - | 60 | | | | 3.1% | 9.2 | AP, CaT, IHC |

A, amiodarone; AP, optical mapping of the action potential; %APD, prolongation percentage of APD; B, β blocker; CaT, optical mapping of calcium transient; CM, cardiomyopathy; CRT, cardiac resynchronization therapy; F, female; LVEF, left ventricular ejection fraction; IHC, immunohistochemical staining; M, male; TCV, transmural conduction velocity; transpl, transplant; VAD, ventricular assist device